GNSS zenith delays and gradients in the analysis of VLBI Intensive sessions

Kamil Teke (1), Johannes Böhm (2), Matthias Madzak (2), Younghee Kwak (2), Peter Steigenberger (3)

(1) Department of Geomatics Engineering, Hacettepe University, Ankara, Turkey; kteke@hacettepe.edu.tr

(2) Department of Geodesy and Geoinformation, Technische Universität Wien, Vienna, Austria; Johannes.Boehm@geo.tuwien.ac.at; Matthias.Madzak@geo.tuwien.ac.at; younghee.kwak@geo.tuwien.ac.at

(3) German Space Operations Center, Deutsches Zentrum für Luft- und Raumfahrt, Oberpfaffenhofen, Germany; peter.steigenberger@dlr.de

Abstract

Very Long Baseline Interferometry (VLBI) is the only space geodetic technique which is capable of estimating Universal Time (UT1=UTC+$\triangle$UT1). So-called VLBI Intensive sessions of the International VLBI Service for Geodesy and Astrometry (IVS) are dedicated to the rapid production of $\triangle$UT1. However, the accuracy achieved with those sessions is still below what could be expected from formal uncertainties of the estimates and one of the reasons is the inappropriate modelling of azimuthal asymmetries of the troposphere delays, because usually no gradients are modelled or estimated. To overcome that deficiency, we introduced troposphere zenith delays and horizontal total gradients estimated from the observations of Global Navigation Satellite Systems (GNSS) i.e. the solution of the Center for Orbit Determination in Europe (CODE) in the analysis of VLBI Intensive sessions carried out from the beginning of 2008 till the end of 2014. We compared our results with the GNSS-derived length-of-day (LOD) estimates of CODE and the International GNSS Service (IGS) and find slight improvements of agreement by up to 1 µsec for both INT1 and INT2 sessions with gradients from CODE. We do not see any additional significant improvement of LOD agreement when GNSS zenith delays are introduced.

1. Introduction

Troposphere delay modeling is a major error source in the analysis of space geodetic observations at radio frequencies, e.g. from the Global Navigation Satellite Systems (GNSS) and geodetic Very Long Baseline Interferometry (VLBI). Usually, the troposphere total delay of the observable is modelled as (Davis et al. 1993)

$$(1) \qquad SD(\varepsilon,\alpha)=ZHD\cdot mf_h(\varepsilon)+ZWD\cdot mf_w(\varepsilon)+mf_g\cdot(G_n\cdot\cos\alpha+G_e\cdot\sin\alpha).$$

The total slant delay SD at an elevation angle ε and azimuth α is the sum of a hydrostatic delay and a wet delay, and each of them is the product of a zenith delay and the corresponding mapping

function. While the zenith hydrostatic delay can be calculated very accurately with the pressure at the antenna and approximate station coordinates following the formula by Saastamoinen (1972) as revised by Davis et al. (1985), the zenith wet delays are usually estimated in the analysis of space geodetic observations as unknown parameters. Furthermore, north and east horizontal total gradients, G_n and G_e, are also estimated in the analysis to account for azimuthal asymmetries in the troposphere delays. The gradient mapping function mf_g times the cosine and the sine of the azimuth serves as partial derivative to determine the gradients in the least-squares adjustment. Usually, the formulation by Davis et al. (1993) as modified by MacMillan (1995) or the equation by Chen and Herring (1997) with C=0.0032 as gradient mapping function are applied. For more information about troposphere delay modelling in space geodesy we refer to an overview paper by Nilsson et al. (2013).

In contrast to VLBI 24 h sessions with about six or more participating stations, gradients are usually not estimated in the analysis of Intensive sessions of the International VLBI Service for Geodesy and Astrometry (IVS; Schuh and Behrend 2012) with just two or three stations observing for one or two hours with the sole purpose to determine Universal Time $\triangle$UT1 (UT1-UTC). The so-called INT1 sessions (Intensives 1) are usually observed from Monday to Friday at about 18 UT on the baseline Wettzell (Germany) to Kokee (Hawaii, U.S.A.). Sometimes, also station Svetloe (Russia) joins the observations, and for several weeks, the baseline Wettzell to Kokee was replaced by the baseline Wettzell to Tsukuba (Japan) or Kokee to Ny-Ålesund (Spitsbergen, Norway). Additionally, the INT2 sessions (Intensives 2) are observed on the baseline Wettzell to Tsukuba at about 7 UT on Saturdays and Sundays and on Mondays INT3 sessions (Intensives 3) are observed including Ny-Ålesund (Luzum and Nothnagel 2010) with frequent participation by Seshan (China). The baseline geometry of the INT1 and INT2 sessions is shown in Figure 1. The projection of the baseline onto the equatorial plane needs to be long to sustain high sensitivity of the VLBI observations to $\triangle$UT1 (Nothnagel and Schnell 2008; Nilsson et al. 2011). However, long baselines of the IVS Intensive sessions limit the number of sources to be observed simultaneously by both antennas resulting in poor sky coverage. This is in contradiction to the fact that a homogeneous distribution of the observations in the sky is essential for a realistic zenith wet delay and gradient estimation at the corresponding station which is required for the accurate determination of $\triangle$UT1 from Intensive sessions. Due to the fact that GNSS observations have a much better sky coverage compared to VLBI Intensive sessions we expect a significant accuracy improvement of $\triangle$UT1 from Intensive sessions when GNSS troposphere delays are used for the analysis of Intensive sessions at co-location sites.

Figure 1. Baseline geometry of the VLBI Intensive sessions, INT1 and INT2. The INT1 baseline is plotted in cyan and the INT2 baseline in red (stereographic map projection).

Several accuracy assessments on $\triangle$UT1 observed by the Intensive sessions of the IVS were carried out in the past, e.g. by Robertson et al. (1985), Ray et al. (1995), Hefty and Gontier (1997). However, due to the small number of observations in the Intensive sessions at that time (1984-1996) zenith wet delays could not be estimated. Titov (2000) assessed the effect of nutation models, i.e. IAU 1980 (Wahr 1981) and IERS 1996 (Herring 1996), on $\triangle$UT1 estimates. Baver et al (2004) analyzed IVS INT1 and INT2 sessions observed from July 2002 till December 2003, compared their UT1 estimates with those of 24 hour IVS sessions and IERS C04, and investigated the effects of the observed sources distribution on UT1 formal errors for Intensive sessions. More recently, Nothnagel and Schnell (2008) investigated the propagation of the errors in polar motion and nutation angles on $\triangle$UT1 estimates in the analyses of Intensive sessions. Thaller et al. (2008) found an accuracy improvement of $\triangle$UT1 from Intensive sessions, observed from November 2006 until February 2008, when a combination with GPS solutions at the normal equation level is performed.

While in multi-station networks the average over all troposphere gradients tends to be zero and the impact on estimated Earth orientation parameters is rather small, $\triangle$UT1 from single baselines can be significantly wrong. Böhm and Schuh (2007a) found a systematic change of $\triangle$UT1 by 15 μsec/mm sum of east gradients; on the other hand they stated that the estimation of zenith wet delays is not critical for the accuracy of $\triangle$UT1 since troposphere mapping function errors mainly affect station heights rather than horizontal components and the influence of mapping function errors on $\triangle$UT1 is rather small, i.e. below ± 1.5 μsec. Consequently, they concluded that an improved modelling of azimuthal asymmetries in the troposphere delays is highly desirable for accurate $\triangle$UT1 estimation from the observations of Intensive sessions.

Böhm and Schuh (2007b) derived gradients from refractivity profiles along the site verticals and found improved accuracies compared to zero gradients in the analysis of 24 h VLBI sessions. Böhm et al. (2010) and Nafisi et al. (2012) applied ray-traced delays in the analysis of Intensive 2 sessions and found a slight improvement when comparing length-of-day values from adjacent Intensive sessions to those derived from GNSS. Nilsson et al. (2011) demonstrated that the accuracy of Intensive sessions can be improved when using external information about the gradients or when estimating gradients using 2 h single baseline sessions during the IVS-CONT08 campaign. Nilsson et al. (2014) found weighted root mean square differences between VLBI and GNSS LOD estimates from 2010 until 2012 with values of 16.4 μsec for IVS-R1 sessions and 21.4 μsec for IVS-R4 sessions. On the other hand, they found smaller weighted root mean square differences between GNSS LOD and VLBI estimates from CONT08 and CONT11 campaigns with values of 8.0 μsec and 6.8 μsec, respectively. The better agreement of LOD between VLBI CONT campaigns and GNSS found by Nilsson et al. (2014) is due to the different characteristics of the IVS session types, i.e. CONT

sessions versus Intensive sessions, with CONT sessions including more antennas and radio sources and having a better temporal and spatial distribution of observations. In addition to the troposphere gradients, corrections to the a priori polar motion coordinates and celestial pole offsets can be estimated in the analyses of CONT sessions which at the end results in a better accuracy of LOD from CONT sessions compared to Intensive sessions.

In this study, we used GNSS zenith delays and gradients as derived from the solution of the Center for Orbit Determination in Europe (CODE, Dach et al. 2009) in the analysis of VLBI Intensive sessions, i.e., INT1 and INT2 observed from the beginning of 2008 till the end of 2014. We selected certain Intensive sessions according to the availability of zenith delays and gradients estimated by CODE analyses at co-located GNSS sites. Co-located GNSS and VLBI sites have the same atmosphere conditions at the same observation epochs provided the horizontal distance between the co-located sites is not too long (maximum in this study at Tsukuba with about 300 m, see Table 1) and the troposphere zenith delays are corrected due to the height differences between the co-located antennas (Saastamoinen 1972, Brunner and Rüeger 1992, Teke et al. 2013).

Table 1. ITRF2008 ellipsoidal heights and approximate horizontal distances between co-located VLBI and GNSS antennas which contributed to IVS INT1 and INT2 sessions from the beginning of 2008 till the end of 2014 and are considered in this study along with the mean zenith delay corrections due to height differences between GNSS and VLBI antennas. Co-location sites are ordered according to their latitude from north to south.

Zenith delay corrections due to the atmosphere between co-located GNSS and VLBI antennas were introduced to the zenith delay estimates of GNSS relative to a reference height at the co-location sites. We selected the height of the VLBI antenna reference point as the reference height of the corresponding co-located site. We used the mean values of the zenith delay corrections of a series of continuous IVS campaigns (CONT02, CONT05, CONT08, and CONT11) as reported by Teke et al. (2013) (Table 1, last column) in one of our solutions of Intensive sessions in this study. They introduced zenith delay corrections at co-location sites and quantified the agreement of the zenith delay and gradients derived from various space geodetic techniques and numerical weather models where they calculated zenith hydrostatic delay corrections according to Saastamoinen (1972) and (1973) and wet corrections according to Brunner and Rüeger (1992) using total pressure, water vapor pressure, and temperature values at co-location sites derived from re-analysis data of the European Centre for Medium Range Weather Forecasts (ECMWF) (Dee et al. 2011).

UT1 estimates of Intensive sessions must be available soon after the session observed so as to be useful for UT1 prediction e.g. for near real-time applications. According to Schuh and Behrend

(2012), IVS Intensive sessions i.e. INT1 and INT2 have a latency of one or two days, means that the observation file of an Intensive session is ready for the analysis one or two days after the session observed. On the other hand, CODE ultra-rapid solution has a maximum delay of 3 hours after the observation with the troposphere product delivery at 3:00, 9:00, 15:00, and 21:00 UT. This means that the latencies of the INT1 and INT2 sessions are much larger than the latency of GNSS troposphere delays. Thus, there is not any additional latency of UT1 due to the availability of the GNSS troposphere delays. However, ultra-rapid UT1 experiments which consist e-transferring the VLBI observations, e.g. Matsuzaka et al. (2008), Sekido et al (2008), Haas et al (2010) and Weimin et al (2012), would need near real-time GNSS troposphere delays.

In Section 2, we introduce the parameterization of certain types of solutions of VLBI Intensive sessions observed from the beginning of 2008 till the end of 2014 and the properties of the GNSS zenith delays and gradients estimated at co-location sites from CODE solution that we reduced from VLBI observations of Intensive sessions a priori to the parameter estimation. In Section 3.1 and 3.2, we discuss the impact of externally introduced zenith delays and gradients from the GNSS analyses, i.e. from CODE, on the ΔUT1 estimates of VLBI Intensive sessions. In Section 3.3, we compare ΔUT1 and LOD estimates of our solutions of VLBI Intensive sessions with respect to the IERS C04 08 series and the LOD estimates of the CODE and IGS solutions, respectively. The conclusions are presented in Section 4.

2. Analysis of VLBI Intensive Sessions

We only consider the baseline Wettzell-Kokee for INT1 sessions and Wettzell-Tsukub32 for INT2 sessions in this study. Among the 1575 INT1 sessions planned by the IVS from the beginning of 2008 till the end of 2014, we included only the observations of Wettzell and Kokee antennas in our analyses. During this time span of about seven years, there were 121 INT1 sessions observed with SVETLOE and 23 INT1 sessions with NYALES20. Instead of removing the whole INT1 sessions from the analyses in which Svetloe and Nyales20 took part we excluded the observations of these antennas from the analyses. The IVS planned to observe in total 577 INT2 sessions from the beginning of 2008 till the end of 2014 with only the antennas Wettzell and Tsukub32. On the other hand, 206 INT3 sessions with the observations of Nyales20 and 22 INT3 sessions with the observations of both Nyales20 and Seshan25 are not considered in this study. Moreover, we exclude certain INT1 and INT2 sessions from the analyses due to the following reasons: large a posteriori variance of unit weight compared to the a priori variance, large formal error of UT1 estimate (larger than 30 μsec), unavailability of the GNSS CODE delays around the observations of Intensive sessions (-2.5 hours < middle of the Intensive session < 2.5 hours), large zenith delay and gradient errors estimated from the GNSS CODE solution (GNSS CODE zenith delays and gradients are important since we externally

introduce them into Intensive sessions). After eliminating these Intensive sessions the remaining 1434 INT1 and 451 INT2 sessions with available GNSS CODE delays were included in our analyses. The average number of observations per session is about 20 for INT1 and 38 for INT2 sessions.

We carried out four types of VLBI solutions to quantify the effect of GNSS troposphere delays on $\triangle$UT1 and length-of-day (LOD) estimates of Intensive sessions. For all solutions, we calculated the zenith hydrostatic delay (ZHD_{VLBI}) with total surface pressure values measured at the VLBI sites (Saastamoinen 1972; Davis et al. 1985) and mapped them with the hydrostatic Vienna Mapping Functions 1 (VMF1, Böhm et al. 2006) to get the slant hydrostatic delays. We subtracted the slant hydrostatic delays from each VLBI observation of the Intensive sessions a priori to the parameter estimation. Differences between our solutions are just in terms of zenith delay and gradient parameterizations.

- *Standard solution (Solution 1):* We analyzed the Intensive sessions with a standard Intensive session analysis procedure. In this procedure, one zenith wet delay offset for each VLBI site per session is estimated and gradients are fixed to zero.
- *Solution with gradients from GNSS (Solution 2)*: One zenith wet delay offset for each VLBI site per session is estimated as also done in the *Standard solution (Solution 1).* The difference of this solution from *Solution 1* is that GNSS gradients are included in the analysis of Intensive sessions. In this approach we interpolated total gradients estimated from GNSS solution by CODE to the VLBI observation epochs linearly. We calculated azimuthally asymmetric troposphere delays through mapping the interpolated horizontal total north and east gradients to slant direction using the third term of Equation (1) where the gradient mapping function by Chen and Herring (1997) was used.
- *Solution with zenith wet delays and gradients from GNSS (Solution 3)*: In this solution, zenith wet delays and gradients from the GNSS solution by CODE were included in the analysis of Intensive sessions. Thus, we first interpolated zenith delay and gradient estimates of GNSS to the VLBI observation epochs linearly. Then, we added a mean zenith delay correction (ΔZTD) due to the height differences (Table 1, last column) to ZHD_{VLBI} of each co-located site. The GNSS zenith wet delays at the VLBI height, ZWD_{GNSS}@VLBI for each observation epoch were derived as ZTD_{GNSS}-(ZHD_{VLBI}+ΔZTD). Thereafter, ZHD_{VLBI} and ZWD_{GNSS}@VLBI were mapped to slant elevations using VMF1. The azimuthally asymmetric delays were calculated in the same way as in *Solution 2.* Then, we reduced the total slant delays (sum of azimuthally symmetric and asymmetric delays) from each VLBI observation of the Intensive session a priori to the parameter estimation.

The zenith delay differences due to the atmosphere between co-located antennas might slightly change with respect to the mean values (given in the last column of Table 1) from one Intensive session to another. Thus, we estimated one zenith wet delay offset (which has a very small value in the order of a few millimeters at maximum) for each session to eliminate the residual zenith delays from the observations.

- *Solution with zenith wet delays and gradients from GNSS without height corrections (Solution 4)*: We keep the same parameterization *as in Solution 3* except that neither mean zenith delay corrections are introduced nor zenith wet delays are estimated.

All the other parameterization of these four types of solutions is as follows: We analyzed VLBI Intensives using the Vienna VLBI Software (VieVS, Böhm et al. 2012) Version 2.2, which is developed at the Department of Geodesy and Geoinformation at the Vienna University of Technology. The classical Gauss-Markoff least-squares adjustment method was used for estimating the parameters. We did not exclude any observation below a certain cut off elevation angle nor did we apply elevation dependent down-weighting to the observations. We fixed source coordinates to ICRF2 (International Celestial Reference Frame 2, Fey et al. 2009), nutation offsets to IAU2000A nutation model plus IERS C04 08 corrections (Bizouard and Gambis 2009) and polar motion coordinates to IERS C04 08 plus high-frequency tidal terms modeled as recommended by the IERS Conventions 2010 (Petit and Luzum 2010). One constant ΔUT1 offset for each Intensive session was estimated with respect to IERS C04 08. We fixed antenna coordinates to the VieTRF13b catalogue (Krásná et al. 2014). Tidal and non-tidal atmospheric loading corrections (Petrov and Boy 2004), tidal ocean loading corrections based on the ocean model FES2004 (Lyard et al. 2006), pole tide and ocean pole tide corrections (Petit and Luzum 2010) were introduced to the antenna coordinates for each observation a priori to the parameter estimation. One offset and a rate between the clocks were estimated.

The CODE zenith delays and gradients used in this study were computed with the Bernese GNSS Software version 5.3 (Dach et al. 2007). They are obtained from the CODE contribution to the 2nd IGS reprocessing campaign (repro2). The general processing strategy is discussed in Steigenberger et al. (2006) and Steigenberger et al. (2011). Full information about the models and processing strategies used for the CODE contribution to repro2 is given in the CODE Analysis Strategy Summary for IGS repro2[1]. Troposphere zenith delays and gradients were estimated in a global GPS/GLONASS double difference solution together with station coordinates, GNSS satellite orbits, and Earth rotation parameters. CODE provided two different solutions for IGS repro2: a pure 1-day

[1] ftp://ftp.unibe.ch/aiub/REPRO_2013/CODE_REPRO_2013.ACN

solution (co2) and a 3-day solution (cf2). The results presented in this paper are based on the 1-day solution.

Hydrostatic a priori zenith delays were obtained from 6-hourly global grids from ECMWF. A linear interpolation regarding time, latitude, and longitude was applied and the resulting zenith hydrostatic delay was extrapolated from the grid height to the actual station height according to Kouba (2008). Troposphere zenith wet delays and gradients were estimated as a piece-wise linear function with 2 and 24 hour parameter spacing, respectively. The wet VMF1 was used for the estimated zenith wet delays and the mapping function of Chen and Herring (1997) for the gradients. Elevation-dependent weighting with $\sin^2\varepsilon$ and a 3° cut off angle were applied.

LOD from the CODE solution was estimated in the CODE repro2 contribution as one LOD parameter per day. Due to correlations with the orbital elements, satellite techniques like GNSS are not able to determine $\triangle$UT1 (Rothacher et al. 1999). However, the first derivative of $\triangle$UT1, namely LOD, can be estimated from GNSS observations. Therefore, the first $\triangle$UT1 value at 0:00 UT was fixed to IERS C04 08 and the second value at 24:00 UT was estimated as piece-wise linear function, i.e., only LOD was estimated. Diurnal and semidiurnal variations in $\triangle$UT1 as well as the $\triangle$UT1 libration were considered according to Petit and Luzum (2010).

The LOD product of IGS, used for the statistical comparisons of this study, are estimated at daily epochs (12 UT) from the weekly combined solutions of IGS analyses centers (AC). The IGS LOD formal uncertainties from the combination is found about 5 μsec. In terms of external comparisons the standard deviation of the combined IGS LOD with respect to the IERS Bulletin A for GPS weeks 1400-1476 is calculated as ±10 μsec, as concluded by Ferland and Piraszewski (2009).

3. Results

In this section, we investigated the effect of externally introduced GNSS (CODE) zenith wet delays and gradients on the ΔUT1 estimates of Intensive sessions. Then, we present the comparison results of LOD estimates between our solutions of Intensive sessions and those of IERS C04 08 and the LOD from the CODE and IGS solutions.

3.1 The effect of GNSS zenith wet delays on ΔUT1 estimates of Intensive sessions

The standard deviations of zenith wet delay differences between GNSS CODE and Solution 1 of VLBI Intensive sessions are 7.5 mm and 7.6 mm at Wettzell and Kokee for INT1 and 4.2 mm and 7.4 mm at Wettzell and Tsukub32 for INT2 from the beginning of 2008 till the end of 2014 (Figure 2). Due to the seasonal large variations and rapidly changing humidity at Tsukuba where the mean zenith wet delay

is about 137 mm and the standard deviation 105 mm, the mean bias and standard deviation of the zenith wet delay differences between Solution 1 of VLBI INT2 and GNSS CODE is -1.0 ± 7.4 mm. We recommend the reader to see the zenith wet delay time series of GNSS CODE and Solution 1 of VLBI INT2 at Tsukuba provided in the supplementary material of this paper. While the zenith wet delay mean biases are rather similar for INT1 and INT2 at Wettzell there is a large difference of standard deviations of about 3.3 mm (7.5 mm - 4.2 mm) (Figure 2).

Figure 2. Biases (white bars) and standard deviations (black and grey bars) of the zenith wet delay (ZWD) differences (∆ZWD) between GNSS CODE and VLBI by site from the beginning of 2008 till the end of 2014. Mean zenith wet delays and their standard deviations are shown in red. The zenith wet delays from VLBI were estimated by Solution 1.

In contrast to Tsukuba and Wettzell a seasonal variation cannot be seen at Kokee in the zenith wet delay time series. The zenith wet delays at Wettzell and Kokee extend up to approximately 200 mm whereas at Tsukub32 they reach up to about 400 mm. Zenith wet delay differences at VLBI observation epochs of Intensive sessions between GNSS CODE and VLBI INT1 can be as large as ±20 mm at all co-located sites of this study (see supplementary material).

The zenith wet delay differences between the estimates of *Solution 2* (*Solution with gradients from GNSS, i.e. CODE*) and GNSS CODE at Kokee (kokb) and Wettzell (wtzr) co-location sites mostly vary within ±4 mm while ΔUT1 differences between *Solution 2* and *Solution 3* vary within ±10 µsec (Figure 3). The linear correlation between zenith wet delay and ΔUT1 differences is found to be nearly negligible. On the other hand, zenith wet delays are highly correlated with other parameters like clock estimates; thus, we find that the variation of ΔUT1 estimates with zenith wet delay changes can increase up to a 20 µsec level (Figure 3).

Figure 3. Station wise zenith wet delay differences per INT1 session between the estimates of Solution 2 and GNSS CODE *versus ΔUT1 differences between Solution 2 (Solution with zenith wet delays estimated, gradients from GNSS CODE) and Solution 3 (Solution with both zenith wet delays and gradients from GNSS CODE). The lines are linear polynomial fits to the scattered data.*

3.2 The effect of GNSS gradients on ΔUT1 estimates of Intensive sessions

The standard deviations of GNSS CODE east and north gradients are largest at Tsukuba (tskb) with the values of 0.5 and 0.6 mm, respectively. The mean biases of gradients from GNSS CODE range from -0.5 to 0 mm for all sites during INT1 and INT2 sessions. We found standard deviations and

mean biases of east gradients for INT2 slightly smaller than those of north gradients for both wtzr and tskb sites (Table 2).

Table 2. Mean biases and standard deviations of north and east gradients (G_n and G_e) estimated from GNSS CODE solution in mm.

East troposphere gradients at the observing stations reveal a clear linear impact on ΔUT1 estimates of Intensive sessions as shown in the left plot of Figure 4. When GNSS CODE gradients are introduced a priori to the VLBI observations of Intensive sessions (*Solution 2*) the effect of the sum of east gradients over the stations on ΔUT1 estimates of INT1 sessions (Wettzell-Kokee) is 12.9 μsec/mm (inferred from the rate of the linear fit to the black plus signs scattered in the left plot of Figure 4) and for the INT2 sessions (Wettzell-Tsukuba) it is 10.7 μsec/mm. Böhm and Schuh (2007a) and Nilsson et al. (2011) found similar results of ΔUT1 change by 15 μsec/mm and 10 to 12 μsec/mm sum of east gradients after their analyses of VLBI Intensive sessions, respectively. As expected, we could not find a significant linear impact of the sum of north gradients over the stations on ΔUT1 estimates when CODE gradients are a priori introduced in the analyses of both INT1 and INT2 sessions carried out from the beginning of 2008 till the end of 2014 (right plot of Figure 4, see also the supplementary material for INT2).

Figure 4. Sum of total east (black plus signs) and north gradients (red crosses) from CODE over the observed stations which are included in Solution 2 versus $\triangle$UT1 differences between Solution 1 (Standard solution: gradients fixed to zero) and Solution 2 (Solution with gradients from GNSS CODE) for INT1 sessions.

3.3 ΔUT1 and length-of-day (LOD) comparisons

When we compared ΔUT1 estimates from our solutions of Intensive sessions with those of IERS C04 08 a slight improvement of ΔUT1 agreement in biases and standard deviations is found for the INT1 Intensive sessions when GNSS gradients from CODE solutions were introduced and zenith wet delays are estimated (*Solution 2*) compared to the standard solution (*Solution 1*) (Table 3). However, since ΔUT1 estimates from Intensive sessions are mainly used for the production of IERS C04 08 series, comparisons of estimated ΔUT1 with IERS C04 08 series may not be the best way of assessing ΔUT1 accuracy improvement.

Table 3. Biases and standard deviations of ΔUT1 in μsec between IERS C04 08 and those estimated from our solutions of VLBI Intensive sessions, i.e. INT1 and INT2, observed from the beginning of 2008 till the end of 2014. The a priori EOP series was set to IERS C04 08 when analyzing the sessions. The

total number of ΔUT1 values used for the bias and standard deviation calculations is given in parentheses. ∆UT1 median formal errors of all Intensive solutions are written in μsec in brackets.

LOD estimates from GNSS are independent of VLBI (Dow et al. 2009). A better assessment of the accuracy improvement of ΔUT1 with GNSS slant delays is realized by comparing length-of-day (LOD) estimates from Intensives with LOD from GNSS. Thus, LOD estimates from independent GNSS solutions, i.e. CODE and IGS, were considered for comparisons. We compared LOD estimated from our solutions of VLBI Intensives with those from CODE and IGS solutions in terms of calculating standard deviations of the LOD differences. We calculated LOD from the estimated ΔUT1 values of INT1 and INT2 sessions with

$$\text{LOD}(t_0)=\left(\frac{\Delta\text{UT1}(t_2)-\Delta\text{UT1}(t_1)}{t_2-t_1}\right)\cdot 1\,\text{day} \qquad (t_2-t_1<1.2\,\text{day}) \tag{2}$$

where t_1 and t_2 are the consecutive estimation epochs of ΔUT1 and t_0 denotes the epoch of LOD and is calculated as $(t_1+t_2)/2$. The daily LOD values from CODE and IGS solutions and IERS C04 08 series were interpolated to the LOD epochs of INT1 and INT2 VLBI Intensive sessions using Lagrange interpolation. We calculated LOD formal errors (shown in Table 4 in brackets) from those of ∆UT1 following the general law of propagation of variances:

$$\sigma_{LOD(t_0)}=\frac{\sqrt{\sigma_{\Delta\text{UT1}(t_1)}^{\,2}+\sigma_{\Delta\text{UT1}(t_2)}^{\,2}}}{t_2-t_1}. \tag{3}$$

We found a slight improvement of LOD agreement in standard deviation of LOD differences between *Solution 2* (*Solution with gradients from GNSS*) and GNSS CODE and IGS solutions compared to *Solution 1* (*Standard solution*) by up to 1 μsec when CODE troposphere gradients are introduced (Table 4).

As we expected, the agreement of LOD from *Solution 4* (*Solution with zenith wet delays and gradients from GNSS without height corrections*) with those of CODE, IGS and IERS C04 08 got worse compared to *Solution 1, Solution 2,* and *Solution 3* for both INT1 and INT2 sessions (Table 4).

Table 4. Biases and standard deviations of LOD differences in μsec between the estimates of VLBI Intensive sessions (INT1 and INT2) and those derived from the solutions of CODE, IGS and IERS C04 08. The total number of LOD used for the standard deviation calculations is given in parentheses. LOD median formal errors of the VLBI Intensive solutions are written in brackets.

When overall biases and standard deviations of LOD differences between the Intensive sessions and GNSS Solutions are considered, INT2 sessions reveals a better agreement than INT1 with GNSS solutions (CODE and IGS) and IERS C04 08. The mean biases and standard deviations of the LOD differences between CODE - IGS, CODE - IERS C04 08, and IGS – IERS C04 08 are found as -12.6 ± 13.3, -10.7 ± 12.3, and 1.3 ± 6.2 μsec, respectively. We get the best agreement of LOD, in standard deviation of LOD differences, between Solution 2 (when zenith wet delays are estimated and gradients are introduced from GNSS CODE in the analysis) of INT2 sessions and GNSS IGS with a standard deviation of 21.3 μsec. The second best agreement of LOD, in standard deviation of LOD differences, is found between Solution 2 of INT2 sessions and IERS C04 08 series with a standard deviation of 21.5 μsec. Considering INT1 sessions, the smallest standard deviation of the LOD differences is found between Solution 3 and IGS with the value of 28.3 μsec. When GNSS CODE zenith wet delays are introduced in Solution 3 to the observations of INT2 sessions, LOD agreement gets slightly worse relative to Solution 2 even though the agreement is better than for Solution 1. Compared to *Solution 1* (*Standard solution*) we obtain a slight improvement of LOD agreement about 1 μsec in the standard deviations of LOD differences with those of CODE, IGS, and IERS C04 08 when troposphere gradients from CODE are introduced into the analyses of Intensive sessions (*Solution 2*).

4. Conclusions

At co-location sites with GNSS, we derived zenith wet delays and troposphere horizontal gradients at each VLBI observation epoch from GNSS CODE solution and introduced them in the analysis of VLBI Intensive sessions observed from the beginning of 2008 till the end of 2014. When we introduce CODE gradients a priori to the analyses of Intensive sessions, there is a linear effect of sum of total east gradients over the stations on ΔUT1 estimates of INT1 sessions (Wettzell-Kokee) of about 13 μsec/mm and of about 11 μsec/mm for INT2 sessions (Wettzell-Tsukuba). Compared to $\triangle$UT1 values from IERS C04 08 series, there is no improvement for INT2 sessions in standard deviations when introducing external troposphere delays from GNSS CODE and only a small improvement in both biases and in standard deviations for INT1 sessions, which is due to that fact that $\triangle$UT1 values of the IERS C04 08 series heavily depend on $\triangle$UT1 values from VLBI Intensive sessions derived without external delays.

We get the best agreement of LOD in standard deviation of differences between IGS LOD and the Intensive session solution when zenith wet delays are estimated and gradients from GNSS CODE are introduced in the analyses of INT2 Intensive sessions. We found a slight improvement of agreement in standard deviation of LOD differences between the Intensive session solution when gradients from CODE are used and GNSS solutions (CODE and IGS) for both INT1 and INT2 sessions. The

improvement is as large as 1 µsec. We do not see any additional significant improvement of LOD agreement when external zenith wet delays are introduced. In conclusion, we suggest that zenith wet delays should be estimated in the analysis of Intensive sessions and either troposphere gradients from the analyses of GNSS observations at co-location sites should be introduced or gradients should be estimated to improve the accuracy of $\triangle$UT1 and LOD estimates of INT1 and INT2 sessions. An improved modelling of azimuthal asymmetries in the troposphere delays is essential for accurate $\triangle$UT1 estimation from the observations of Intensive sessions.

Acknowledgements

This work is supported by the Austrian Science Fund (FWF) with projects P25320-N19 (Radiate VLBI) and M1592 (Hybrid GPS-VLBI). The authors want to acknowledge the International VLBI Service for Geodesy and Astrometry (IVS, Schuh and Behrend 2012), the International GNSS Service (IGS, Dow et al. 2009), the Centre for Orbit Determination in Europe (CODE, Dach et al. 2009), and the European Centre for Medium-Range Weather Forecast (ECMWF, Dee et al. 2011) for providing data.

References

Baver K, MacMillan D, Petrov L, Gordon D (2004) Analysis of the VLBI Intensive Sessions. IVS 2004 General Meeting Proceedings, NASA/CP-2004-212255, 394–398. http://ivscc.gsfc.nasa.gov/publications/gm2004/baver

Bizouard C, Gambis D (2009) The combined solution C04 for Earth orientation parameters consistent with International Terrestrial Reference Frame. In: Drewes H (ed) Geodetic reference frames. IAG Symp, vol 134, pp 265–270. doi:10.1007/978-3-642-00860-3_41

Böhm J, Werl B, Schuh H (2006) Troposphere mapping functions for GPS and very long baseline interferometry from European Centre for Medium-Range Weather Forecasts operational analysis data, J. Geophys. Res. 111, B02406. doi:10.1029/2005JB003629

Böhm J, Schuh H (2007a) Forecasting data of the troposphere used for IVS intensive sessions. In: Böhm J, Pany A, Schuh H (eds) Proceedings of the 18th European VLBI for geodesy and astrometry working meeting, Vienna, 12–13 April 2007, pp 153–157.

Böhm J, Schuh H (2007b) Troposphere gradients from the ECMWF in VLBI analysis. J. Geod 81 (6–8), 403–408. doi:10.1007/s00190-007-0144-2

Böhm J, Hobiger T, Ichikawa R, Kondo T, Koyama Y, Pany A, Schuh H, Teke K (2010) Asymmetric tropospheric delays from numerical weather models for UT1 determination from VLBI Intensive sessions on the baseline Wettzell-Tsukuba, J. Geod. 84 (5), 319-325. doi:10.1007/s00190-10-0370-x

Böhm J, Böhm S, Nilsson T, Pany A, Plank L, Spicakova H, Teke K, Schuh H (2012) The new Vienna VLBI Software VieVS, in Proceedings of IAG Scientific Assembly 2009, International Association of Geodesy Symposia Series Vol. 136, edited by S. Kenyon, M. C. Pacino, and U. Marti, p. 1007-1011, doi:10.1007/978-3-642-20338-1_126

Brunner FK, Rüeger JM (1992) Theory of the local scale parameter method for EDM. Bull. Géod. 66 (4), 355–364. doi:10.1007/BF00807420

Chen G, Herring TA (1997) Effects of atmospheric azimuthal asymmetry on the analysis from space geodetic data. J. Geophys. Res. 102 (B9), 20489–20502. doi:10.1029/97JB01739

Dach R, Hugentobler U, Fridez P, Meindl M (eds) (2007) Bernese GPS Software Version 5.0, Astronomical Institute, University of Bern

Dach R, Brockmann E, Schaer S, Beutler G, Meindl M, Prange L, Bock H, Jäggi A, Ostini L (2009) GNSS processing at CODE: status report. J. Geod. 83 (3–4), 353–365. doi:10.1007/s00190-008-0281-2

Davis JL, Herring TA, Shapiro II, Rogers AEE, Elgered G (1985) Geodesy by Radio Interferometry: Effects of Atmospheric Modeling Errors on Estimates of Baseline Length, Radio Science, Vol. 20 (6), 1593-1607. doi:10.1029/RS020i006p01593

Davis JL, Elgered G, Niell AE, Kuehn CE (1993) Ground-based measurements of gradients in the “wet” radio refractivity of air. Radio Sci. 28 (6), 1003-1018. doi:10.1029/93RS01917

Dee D, Uppala S, Simmons A, Berrisford P, Poli P,Kobayashi S,Andrae U, Balmaseda M, Balsamo G, Bauer P, Bechtold P, Beljaars A, van de Berg L, Bidlot J, Bormann N, Delsol C, Dragani R, Fuentes M, Geer A, Haimberger L, Healy S, Hersbach H, Holm E, Isaksen L, Kallberg P, Köhler M, Matricardi M, McNally T, Monge-Sanz B, Morcrette JJ, Park BK, Peubey C, de Rosnay P, Tavolato C, Thépaut JN, Vitart F (2011) The ERA-Interim reanalysis: configuration and performance of the data assimilation system. Q. J. R. Meteorol. Soc. 137, 553–597. doi:10.1002/qj.828

Dow JM, Neilan RE, Rizos C (2009) The International GNSS Service in a changing landscape of Global Navigation Satellite Systems. J. Geod. 83 (3-4), 191–198. doi:10.1007/s00190-008-0300-3

Ferland R, Piraszewski M (2009) The IGS-combined station coordinates, earth rotation parameters and apparent geocenter. J. Geod. 83, 385-392, doi: 10.1007/s00190-008-0295-9

Fey A, Gordon D, Jacobs CS (2009) The second realization of the International Celestial Reference Frame by very long baseline interferometry. IERS Technical Note, vol 35. Verlag des Bundesamts für Kartographie und Geodäsie, Frankfurt am Main, ISBN 3-89888-918-6

Haas R, Sekido M, Hobiger T, Kondo T, Kurihara S, Tanimoto D, Kokado K, Wagner J, Ritakari J, Mujunen A (2010) Ultra-Rapid DUT1-Observations with E-VLBI. Artificial Satellites, 45, No. 2 doi: 10.2478/v10018-010-0007-6

Hefty J, Gontier AM (1997) Sensitivity of UT1 determined by single baseline VLBI to atmospheric delay model, terrestrial and celestial reference frames. J. Geod. 71 (5), 253–261. doi: 10.1007/s001900050093

Herring TA (1996) The IERS 1996 theory of precession/nutation. In: McCarthy DD (ed.) IERS Conventions (1996), IERS Technical Note 21, Observatoire de Paris, pp 25-32

Kouba J (2008) Implementation and testing of the gridded Vienna Mapping Function 1 (VMF1). J. Geod. 82 (4-5), 193-205. doi: 10.1007/s00190-007-0170-0

Krásná H, Böhm J, Plank L, Nilsson T, Schuh H (2014) Atmospheric Effects on VLBI-Derived Terrestrial and Celestial Reference Frames, Earth on the Edge: Science for a Sustainable Planet Proceedings of the IAG General Assembly, Melbourne, Australia, June 28 - July 2, 2011, Series: International Association of Geodesy Symposia, Vol. 139, edited by Chris Rizos and Pascal Willis, pp. 203-208, doi:10.1007/978-3-642-37222-3_26

Luzum B, Nothnagel A (2010) Improved UT1 predictions through low latency VLBI observations. J. Geod. 84 (6), 399–402. doi:10.1007/s00190-010-0372-8

Lyard F, Lefevre F, Lettelier T, Francis O (2006) Modelling the global ocean tides, Modern insights from FES2004. Ocean Dyn. 56 (6), 394–415. doi:10.1007/s10236-006-0086-x

MacMillan DS (1995) Atmospheric gradients from very long baseline interferometry observations. Geophys. Res. Lett. 22(9), 1041–1044. doi:10.1029/95GL00887

Matsuzaka S, Shigematsu H, Kurihara S, Machida M, Kokado K, Tanimoto D (2008) Ultra rapid UT1 experiment with e-VLBI. In: Finkelstein A, Behrend D (eds) Proceedings of the fifth IVS general meeting: measuring the future, pp 68–71. http://ivscc.gsfc.nasa.gov/publications/gm2008/

Nafisi V, Madzak M, Böhm J, Ardalan AA, Schuh H (2012) Ray-traced tropospheric delays in VLBI analysis, Radio Science 47, RS2020. doi:10.1029/2011RS004918

Nilsson T, Böhm J, Schuh H (2011) Universal time from VLBI single-baseline observations during CONT08, J. Geod. 85 (7), 415-423. doi:10.1007/s00190-010-0436-9

Nilsson T, Böhm J, Wijaya DD, Tresch A, Nafisi V, Schuh H (2013) Path Delays in the Neutral Atmosphere, in: Johannes Böhm and Harald Schuh (eds): Atmospheric Effects in Space Geodesy, Springer Verlag, ISBN 978-3-642-36931-5, pp. 73-136. doi:10.1007/978-3-642-36932-2_3

Nilsson T, Heinkelmann R, Karbon M, Raposo-Pulido V, Soja B, Schuh H (2014) Earth orientation parameters estimated from VLBI during the CONT11 campaign. J. Geod. 88 (5), 491-502. doi:10.1007/s00190-014-0700-5

Nothnagel A, Schnell D (2008) The impact of errors in polar motion and nutation on UT1 determinations from VLBI intensive observations. J. Geod. 82 (12), 863–869. doi:10.1007/s00190-008-0212-2

Petit G, Luzum B (2010) IERS Conventions 2010, IERS Technical Note; 36. Verlag des Bundesamts für Kartographie und Geodäsie, Frankfurt am Main, ISBN 3-89888-989-6

Petrov L, Boy JP (2004) Study of the atmospheric pressure loading signal in very long baseline Interferometry observations. J. Geophys. Res. 109 (B3), B03405. doi:10.1029/2003JB002500

Ray JR, Carter WE, Robertson DS (1995) Assessment of the accuracy of daily UT1 determinations by very long baseline interferometry. J. Geophys. Res. 100 (B5), 8193–8200. doi:10.1029/95JB00151

Robertson DS, Carter WE, Campbell J, Schuh H (1985) Daily Earth rotation determinations from IRIS very long baseline interferometry. Nature 316, 424–427

Rothacher M, Beutler G, Herring TA, Weber R (1999) Estimation of nutation using the Global Positioning System. J. Geophys. Res. 104 (B3), 4835-4859. doi:10.1029/1998JB900078

Saastamoinen J (1972) Atmospheric correction for the troposphere and stratosphere in radio ranging of satellites, in: The use of artificial satellites for geodesy, Geophys. Monogr. Ser. 15, Amer. Geophys. Union, pp. 274-251

Saastamoinen J (1973) Contribution to the theory of atmospheric refraction (in three parts). Bull. Geod. 105–107:279–298

Schuh H, Behrend D (2012) VLBI: a fascinating technique for geodesy and astrometry. J. Geodyn. 61, 68–80. doi:10.1016/j.jog.2012.07.007

Sekido M, Takiguchi H, Koyama Y, Kondo T, Haas R, Wagner J, Ritakari J, Kurihara S, Kokado K (2008) Ultra-rapid UT1 measurements by e-VLBI. Earth Planets and Space 60: 865-870

Steigenberger P, Rothacher M, Dietrich R, Fritsche M, Rülke A, Vey S (2006) Reprocessing of a global GPS network. J Geophys Res 111 (B5), doi:10.1029/2005JB003747

Steigenberger P, Hugentobler U, Lutz S, Dach R (2011) CODE contribution to the IGS reprocessing. Technical Report, Institut für Astronomische und Physikalische Geodäsie, TU München

Teke K, Nilsson T, Böhm J, Hobiger T, Steigenberger P, Espada SG, Haas R, Willis P (2013) Troposphere delays from space geodetic techniques, water vapor radiometers, and numerical weather models over a series of continuous VLBI campaigns, J. Geod. 87 (10), 981-1001. doi:10.1007/s00190-013-0662-z

Thaller D, Tesmer V, Krügel M, Steigenberger P, Dach R, Rothacher M (2008) Combining VLBI intensive with GPS rapid solutions for deriving a stable UT time series. In: Behrend D, Baver KD (eds) International VLBI Service for Geodesy and Astrometry 2008 General Meeting Proceedings, 8–13

Titov O (2000) Influence of adopted nutation model on VLBI NEOS-intensives analysis. Proceedings of the IAU colloquium 180, Towards models and constants for sub-microarcsecond astrometry, 27-30 March 2000, US Naval Observatory, Washington, DC

Wahr JM (1981) The forced nutations of an elliptical, rotating, elastic and oceanless earth. Geophys. J. R. Astron. Soc. 64 (3), 705-727. doi:10.1111/j.1365-246X.1981.tb02691.x

Weimin Z, Zhong C, Li T (2012) e-VLBI Applications of Chinese VLBI Network. VS 2012 General Meeting Proceedings, 99-102. http://ivscc.gsfc.nasa.gov/publications/gm2012/zheng.pdf

TABLES

Table 1. ITRF2008 ellipsoidal heights and approximate horizontal distances between co-located VLBI and GNSS antennas which contributed to IVS INT1 and INT2 sessions from the beginning of 2008 till the end of 2014 and are considered in this study along with the mean zenith delay corrections due to height differences between GNSS and VLBI antennas. Co-location sites are ordered according to their latitude from north to south.

Co-location sites	Latitude (°)	Country	VLBI acronym	Height VLBI site (m)	GNSS site acronym	VLBI-GNSS approximate horizontal distance (m)	Height GNSS site (m)	VLBI-GNSS height difference (m)	VLBI-GNSS mean zenith delay corrections (mm)
Wettzell (wtzr)	49.1	Germany	WETTZELL	669.1	wtzr	139	666.1	3.0	-0.9
Tsukuba (tskb)	36.1	Japan	TSUKUB32	84.7	tskb	302	67.3	17.4	-6.1
Kokee Park (kokb)	22.1	USA	KOKEE	1176.6	kokb	45	1167.4	9.2	-2.7

Table 2. Mean biases and standard deviations of north and east gradients (G_n and G_e) estimated from GNSS CODE solution in mm.

GNSS sites	Biases and standard deviations			
	INT1 sessions		INT2 sessions	
	G_n from $GNSS_{CODE}$	G_e from $GNSS_{CODE}$	G_n from $GNSS_{CODE}$	G_e from $GNSS_{CODE}$
wtzr	-0.2 ± 0.4	0.0 ± 0.4	-0.2 ± 0.4	0.0 ± 0.3
tskb	-	-	-0.4 ± 0.6	0.0 ± 0.5
kokb	-0.5 ± 0.5	-0.2 ± 0.5	-	-

Table 3. Biases and standard deviations of ΔUT1 in μsec between IERS C04 08 and those estimated from our solutions of VLBI Intensive sessions, i.e. INT1 and INT2, observed from the beginning of 2008 till the end of 2014. The a priori EOP series was set to IERS C04 08 when analyzing the sessions. The total number of ΔUT1 values used for the bias and standard deviation calculations is given in parentheses. △UT1 median formal errors of all Intensive solutions are written in μsec in brackets.

Solution Type	INT1 - IERS C04 08 (1434 △UT1 values)	INT2 - IERS C04 08 (451 △UT1 values)
Solution 1	5.0 ± 18.4 [11.4]	2.1 ± 20.3 [7.5]
Solution 2	2.9 ± 18.3 [11.3]	1.2 ± 22.2 [7.5]
Solution 3	3.1 ± 18.3 [11.3]	1.4 ± 22.4 [7.5]
Solution 4	2.8 ± 21.0 [10.9]	2.7 ± 26.2 [8.2]

Table 4. Biases and standard deviations of LOD differences in μsec between the estimates of VLBI Intensive sessions (INT1 and INT2) and those derived from the solutions of CODE, IGS and IERS C04 08. The total number of LOD used for the standard deviation calculations is given in parentheses. LOD median formal errors of the VLBI Intensive solutions are written in brackets.

Solution Type	INT1 - CODE (933)	INT1 - IGS (933)	INT1 - C04 08 (933)	INT2 - CODE (203)	INT2 - IGS (203)	INT2 - C04 08 (203)
Solution 1	14.0 ± 30.7 [16.9]	2.1 ± 29.3	3.4 ± 29.5	11.5 ± 22.8 [10.7]	-0.6 ± 22.1	0.0 ± 22.2
Solution 2	14.0 ± 29.9 [16.9]	2.1 ± 28.5	3.4 ± 28.5	11.2 ± 21.9 [10.6]	-0.9 ± 21.3	-0.3 ± 21.5
Solution 3	13.9 ± 29.7 [16.7]	1.9 ± 28.3	3.2 ± 28.4	11.4 ± 22.2 [10.7]	-0.7 ± 21.6	-0.1 ± 21.8
Solution 4	13.9 ± 31.9 [16.3]	2.0 ± 30.7	3.3 ± 30.8	9.9 ± 24.1 [11.9]	-2.3 ± 23.2	-1.6 ± 23.6

FIGURES

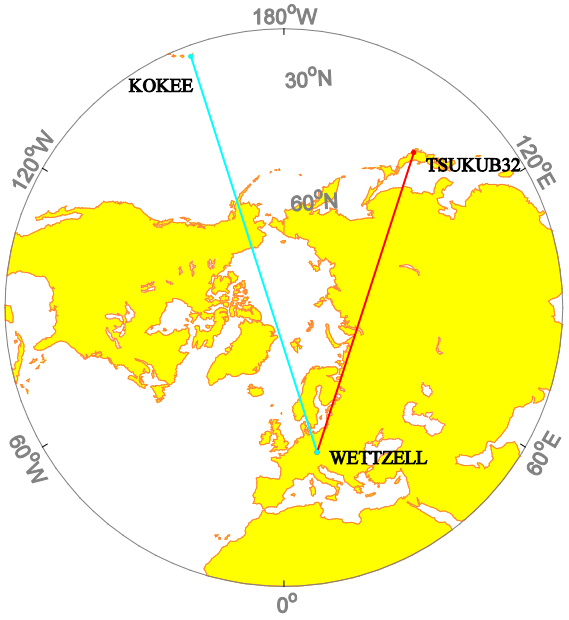

Figure 1. Baseline geometry of the VLBI Intensive sessions, INT1 and INT2. The INT1 baseline is plotted in cyan and the INT2 baseline in red (stereographic map projection).

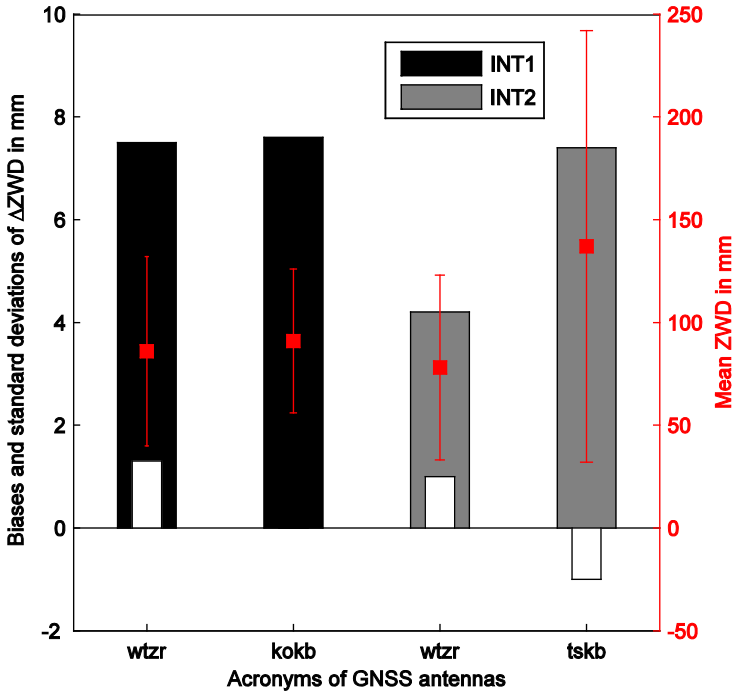

Figure 2. Biases (white bars) and standard deviations (black and grey bars) of the zenith wet delay (ZWD) differences (∆ZWD) between GNSS CODE and VLBI by site from the beginning of 2008 till the end of 2014. Mean zenith wet delays and their standard deviations are shown in red. The zenith wet delays from VLBI were estimated by Solution 1.

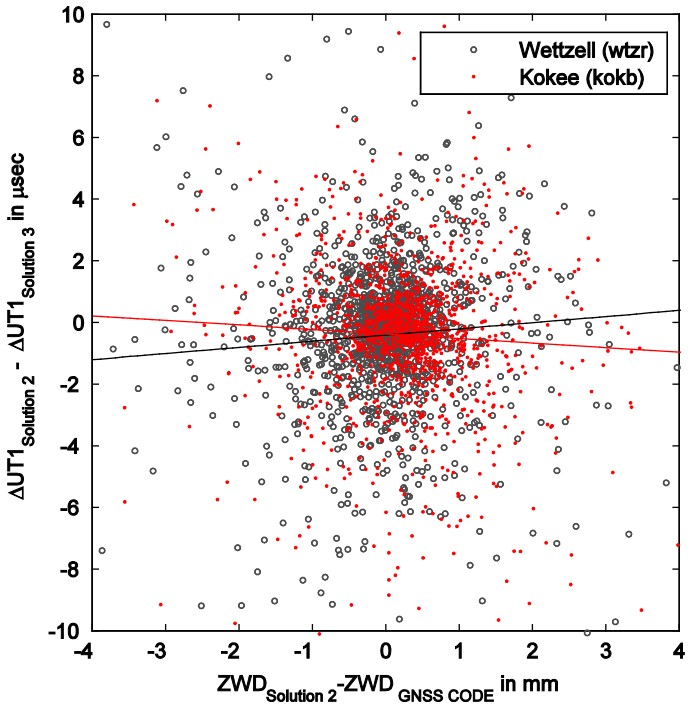

Figure 3. Station wise zenith wet delay differences per INT1 session between the estimates of Solution 2 and GNSS CODE *versus ΔUT1 differences between Solution 2 (Solution with zenith wet delays estimated, gradients from GNSS CODE) and Solution 3 (Solution with both zenith wet delays and gradients from GNSS CODE). The lines are linear polynomial fits to the scattered data.*

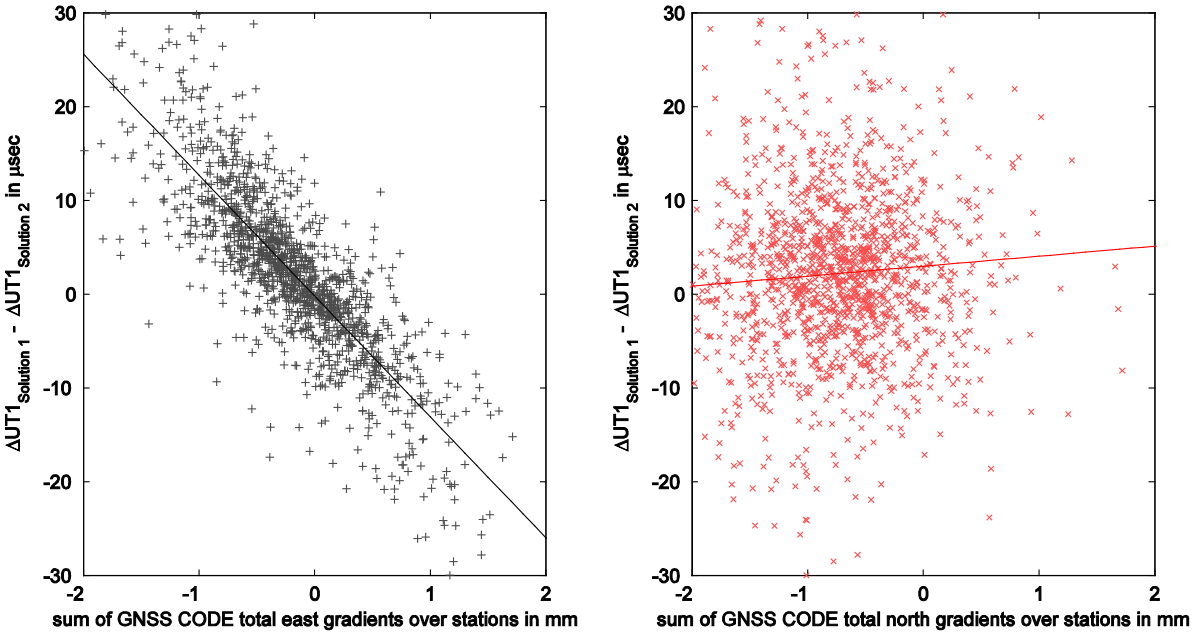

Figure 4. Sum of total east (black plus signs) and north gradients (red crosses) from CODE over the observed stations which are included in Solution 2 versus ∆UT1 differences between Solution 1 (Standard solution: gradients fixed to zero) and Solution 2 (Solution with gradients from GNSS CODE) for INT1 sessions.